

Measurement of Mars Reconnaissance Orbiter Equivalent Isotropic Radiated Power during Early Cruise

D. D. Morabito,¹ D. Lee,¹ M. M. Franco,² and S. Shambayati¹

The X-band (8400- to 8450-MHz) frequency allocation currently used for deep-space telecommunications is not sufficiently wide to accommodate future high-data-rate communication requirements. As a result, future high-rate missions will be transitioning to higher frequency allocations such as Ka-band (31,800 to 32,300 MHz). These higher frequency band allocations are more susceptible to weather effects, resulting in much larger fluctuations in received signal strength than at X-band. A fully functioning Ka-band communications system was implemented on Mars Reconnaissance Orbiter (MRO) and launched in 2005 to develop and demonstrate Ka-band operational concepts and capabilities. This article will discuss activities performed at the DSS-13 34-m-diameter research and development beam-waveguide antenna, conducted primarily for the purpose of characterizing the equivalent isotropic radiated power of the MRO spacecraft during early cruise.

I. Introduction

A fully functioning Ka-band communications system was implemented on Mars Reconnaissance Orbiter (MRO), which was launched on August 12, 2005, from Kennedy Space Center at Cape Canaveral in Florida. The MRO Ka-band (31,800- to 32,300-MHz) subsystem was planned to be used during the mission as a communications demonstration with the goal of developing and refining the Ka-band operations concept for future deep-space missions. In order to test the functional readiness of both the spacecraft and the Deep Space Network (DSN) to support demonstration activities, 10 tracking passes were scheduled and conducted during the mission cruise phase using the DSN 34-m-diameter beam-waveguide (BWG) antennas between September and December 2005. Additional Ka-band tracks were later made available, including some in January 2006. During these passes, the spacecraft and the ground system were put through a series of functional and performance tests, exercising the Ka-band link as well as the concurrent X-band (8400- to 8450-MHz) downlink. An overview of the MRO Ka-band demonstration is provided in [1], and a report of the MRO cruise activities is provided in [2]. This article describes the experiments performed at DSS 13 between September 2005 and January 2006 to characterize the spacecraft equivalent isotropic radiated power (EIRP) and the station Ka-band performance.

¹ Communications Architectures and Research Section.

² Communications Ground Systems Section.

The research described in this publication was carried out by the Jet Propulsion Laboratory, California Institute of Technology, under a contract with the National Aeronautics and Space Administration.

Both the spacecraft's and the DSN's performances were exemplary, with active pointing and blind pointing of the DSN's operational BWG antennas performing well at Ka-band [2]. Among the accomplishments was a record telemetry data return for a deep-space mission realized using MRO Ka-band [2]. However, the spacecraft also presented challenges not normally associated with planetary missions, mostly because of the very high signal power received at the ground. During the cruise phase of the mission, the MRO-to-Earth range was relatively small, and the Ka-band signal was transmitted over the high-gain antenna (HGA) instead of the low-gain antennas (LGAs), since Ka-band could be used only with the HGA. This resulted in a high received signal power, which caused problems with calibration of the HGA antenna pattern and measurement of the in-flight spacecraft EIRP. During September 19–20, 2005, the MRO Project conducted an HGA calibration over Madrid, Spain. During this calibration, the HGA was directed to move its gimbals, causing the antenna beam to sweep over the Earth in two orthogonal directions. The small spacecraft–Earth range caused the received signal strength to saturate the receivers when near on-point, so the antenna pattern could not be adequately measured. In addition, the resolution of the received signal strength data was not adequate to distinguish lobe spacing. The closed-loop receiver used for signal data acquisition could sample down to only 1 Hz, and open-loop receivers were not yet upgraded to accept MRO's Ka-band intermediate frequency (IF), 522 MHz.

As a result of these problems, DSS 13 (a research and development (R&D) 34-m BWG antenna located at Goldstone, California) was utilized in an attempt to measure spacecraft EIRP. This led to the development and exercise of strong-signal EIRP measurement techniques that could be used for future high-power deep-space missions. This article will discuss results using these techniques at DSS 13 on received signals from MRO that spanned the cruise phase from September 2005 to January 2006. These measurements are also compared with similar ones made at the JPL Mesa using two 6-m-diameter prototype breadboard antennas of the DSN Array Project.

II. Early Calibration/Preparation Activities and System Configurations

Among the activities performed at DSS 13 in September and October 2005 were several that involved checkout and calibration of the various subsystems. The dual-frequency X-/Ka-band position at DSS 13 was utilized for most of the tests. In some cases, the X-band feed at the S-/X-band feed position was used to measure and verify MRO's X-band received signal strength. Other activities included characterization and measurement of system operating noise temperature, T_{op} , system gain and linearity, antenna efficiency using natural calibrator radio sources, MRO's X-band signal strength, Cassini's X-band and Ka-band signal strength, Y-factors using hot and cold loads, and follow-on noise temperatures. Tests were also performed in which varying signal power was injected into the front-end to measure linearity and gain, and that exercised pointing techniques and adjustments of attenuator settings to optimize system gain and linearity. The gain differences, ΔG , between the signal paths of the total power radiometer (TPR) (where system gain is obtained from the load calibrations) and the station spectrum analyzer, both relative to the input of the IF distribution rack, were measured.

Gain and linearity calibrations were performed at the beginning of each session or when configuration changes were made. Calibrations were also performed periodically throughout each track in combination with the TPR or station spectrum analyzer measurements. An initial set of calibrations at zenith is always performed at the beginning of a track and sometimes at the end of a track. During each calibration, the TPR measures the total IF noise power while the high electron mobility transistor (HEMT) low-noise amplifier (LNA) input is switched from (1) sky to (2) sky-plus-noise diode to (3) ambient load to (4) ambient-load-plus-noise diode. The measurements are converted into a transfer function (T_{op} versus total noise power) and also allow for the correction of any nonlinearity that may be present. A detailed discussion of the system calibration methodology is provided in [3].

A set of measurements performed early in the effort (September–October 2005) were found to be problematic. Because of the nonavailability of an optimal filter for the TPR for MRO Ka-band (~ 522 -MHz IF), the system was used in an attempt to measure EIRP in a “no-filter” configuration that essentially passed signal and noise energy over the full 500-MHz bandpass of the downconverter to the TPR power meters. With this configuration, the system was measured to have a significant nonlinearity of -10 percent. Another problem encountered with the system was lower than expected power meter readings when using existing narrow-filter configurations at Ka-band for signals near 32 GHz (such as observing Cassini Ka-band or natural radio sources for efficiency). Given that the system was nonoptimal, steps were taken to remedy this. This involved conducting more detailed calibrations of the system as well as procuring a specialized filter to accommodate MRO’s IF frequency at the TPR.

For pointing to the spacecraft, a trajectory file in standard format that covered the period from September 16, 2005, to March 20, 2006 (up to Mars orbit insertion), was received from the MRO navigation team. The state vectors in the trajectory file were interpolated using three points, each separated by an input time interval parameter nominally set to 4 hours. The blind-pointing model used at DSS 13 was usually within 10-mdeg accuracy, but it varied depending on position in the sky inferred from boresight data of the spacecraft and natural radio sources. This was important since DSS 13 does not currently employ any automatic pointing control, such as monopulse. The procedures that were used to fine-tune the pointing at DSS 13 included a manual boresight algorithm tested on Cassini and MRO (X-band and Ka-band), and AUTOBORE,³ a program usually used on wideband natural calibrator radio sources for efficiency measurement purposes. This requires a sufficiently high increase in T_{op} , due to the signal source, which was applicable for MRO X-band and Ka-band during this “near-Earth” phase of the mission.

A. X-Band

The X-band system that was employed at position 1 (X-/Ka-band) in the DSS-13 pedestal room was a dual-polarization package that was installed July 5–8, 2005, to prepare for a Faraday rotation radio science experiment conducted during the solar superior conjunction of the Cassini spacecraft in July 2005.

The AUTOBORE algorithm was successfully performed on the MRO X-band signal on September 28, 2005 (2005/271), providing pointing corrections in two orthogonal directions. This demonstrated the viability of using the AUTOBORE technique on a spacecraft signal, provided sufficient noise temperature increase was available, as was the case for MRO shortly after launch. On the evening of September 28 (2005/271), several attempts to measure the EIRP of the MRO X-band signal were carried out using the station spectrum analyzer, TPR power meter, and Radio Science Receiver (RSR) at DSS 13. The initial measurements of MRO X-band EIRP were found to be lower than predicted. It was suspected that the feed package was not properly aligned with the optics of the BWG. The existing antenna efficiency model for that feed-package position, therefore, was no longer applicable. The degraded efficiency was acceptable for the radio science Faraday rotation experiment, which relies on phase measurements, not signal strength. This led to a need to conduct antenna efficiency measurements at this X-band position (at the X-/Ka-band package) so that the measured MRO signal strength could be properly calibrated. A lateral alignment of the feed horn was performed on November 16, 2005, and additional efficiency data were acquired shortly thereafter to characterize the new configuration.

B. Ka-Band

An initial attempt to measure Ka-band EIRP was performed at DSS 13 on September 24, 2005 (2005/267). During this pass, there were several issues that were addressed or identified, including trajectory file issues, calibration issues, and configuration issues, as well as numerous activities that were in progress. Manual boresight observations were performed using the spectrum analyzer. An initial received signal power measurement performed near the end of the pass did not agree with predicts.

³ The AUTOBORE technique is described in M. Britcliffe, ed., *DSS-13 Beam Waveguide Antenna Project, Phase I Final Report*, JPL D-8451 (internal document), S. Stewart, Chapter 8, Jet Propulsion Laboratory, Pasadena, California, May 15, 1991.

On October 3, 2005 (2005/276), DSS 13 observed the Cassini spacecraft X-band and Ka-band signals in preparation for measuring MRO EIRP. The measured EIRP of Cassini during the one-way ultrastable oscillator (USO) period at the start of the pass agreed with the predicted EIRP. The measurement of the EIRP of Cassini’s three-way coherent Ka-band signal was somewhat more problematic, due to the nature of Cassini’s coherent signal, as the carrier sits upon a pedestal that emerges above the noise floor. As more was learned about this effect,⁴ a refined prediction became available and was found to be in agreement with the measurement. The manual boresight algorithm was tested on Cassini using the power-to-noise ratio measured from the RSR. This method is valid when tracking a “weak” carrier with pure noise background, but it was not expected to work for MRO. Offsets to the blind-pointing model, figured from visual three-point fits during the pass used to correct the pointing, were $\Delta XEL = -3.5$ mdeg (cross-elevation) and $\Delta ELV = +1.0$ mdeg (elevation). An ideal Bessel pattern model was adjusted using these offsets and plotted along with the measured pattern (see Fig. 1). The blind-pointing model at DSS 13 worked well for Cassini for this particular test at the given position in the sky.

On October 19–20, 2005 (2005/292-293), attenuators in the Ka-band downconverter were adjusted to solve gain and linearity issues, and calibrations were performed after each adjustment until suitable system linearity was achieved. The last series of calibrations resulted in a system nonlinearity of -0.95 ± 0.8 percent with 0.12 percent of gain fluctuations for the left-circular polarized (LCP) path. A similar set of adjustments was performed for the right-circular polarized (RCP) path, but a linear system could be achieved only with an unacceptably low power meter reading on ambient load with the noise diode turned on. It was planned to later adjust the attenuator following the mixer in the Ka-band downconverter, and elsewhere in the system. Such adjustments were necessary in order to increase power meter levels using a narrow filter in order to realize a linear system. These refinements were eventually implemented, as well as the addition of an external amplifier in line with the external filter prior to the power meter at the TPR. In addition, attenuation was added in the control room at the output of the fiber optics receiver.

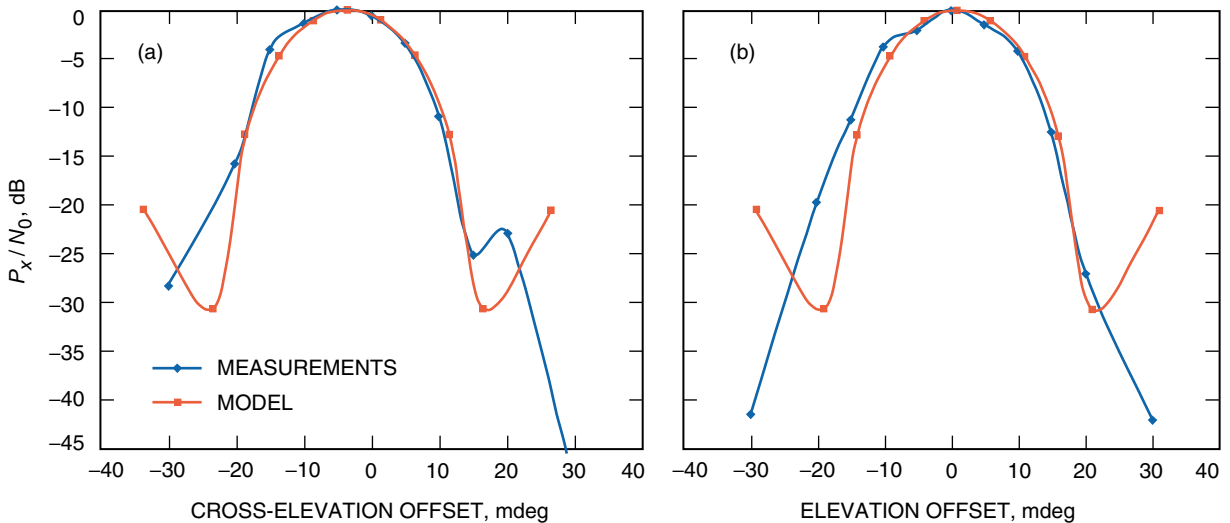


Fig. 1. Measurements of Cassini Ka-band ΔT_{op} relative to sky background converted into relative power units, along with the ideal Bessel pattern adjusted per achieved pointing offsets: (a) cross-elevation and (b) elevation.

⁴Susan Finley and Sami Asmar, Jet Propulsion Laboratory, Pasadena, California, provided needed information on the Cassini coherent Ka-band signal.

III. Antenna Efficiency Measurements

Antenna efficiency measurements using natural calibrator radio sources were performed at both X-band and Ka-band. The objective of these measurements was to obtain updated antenna efficiency versus elevation-angle curves to be used to convert Ka-band received signal strength to spacecraft EIRP. The techniques employed are described in [4]. Most efficiency measurements involved the use of radio source M87 (+12° 23' declination). A higher declination calibrator source, DR21 (+42° 09' declination) was also observed to provide antenna efficiency above an 80-deg station elevation angle. MRO's declination during cruise lay in between the declination of these two natural radio sources. For example, on December 16, 2005 (2005/350), MRO was at a declination of +19° 14'.

A. Ka-Band

Ka-band antenna efficiency measurement sessions were conducted on October 4, 2005 (2005/277), October 12–13, 2005 (2005/285–286), October 26–27 (2005/299–300), and December 13, 2005 (2005/347). The Ka-band antenna efficiency measurements as a function of elevation angle depicted in Fig. 2 appear to peak between 50 deg to 60 deg, away from the expected rigging angle (elevation angle = 45 deg), and also display a “hysteresis” signature between source rise and source set for M87. As a result, a set of different efficiency curves was estimated as well as a mean efficiency curve derived from an average of the DR21 and M87 polynomial coefficients (green curve in Fig. 2).

B. X-Band

The efficiency curve for the X-band package⁵ at the S-/X-band feed (position 2) was used whenever X-band measurements were performed using this package. Antenna efficiency measurements were acquired for X-band at the X-/Ka-band feed position in order to better estimate spacecraft EIRP from received

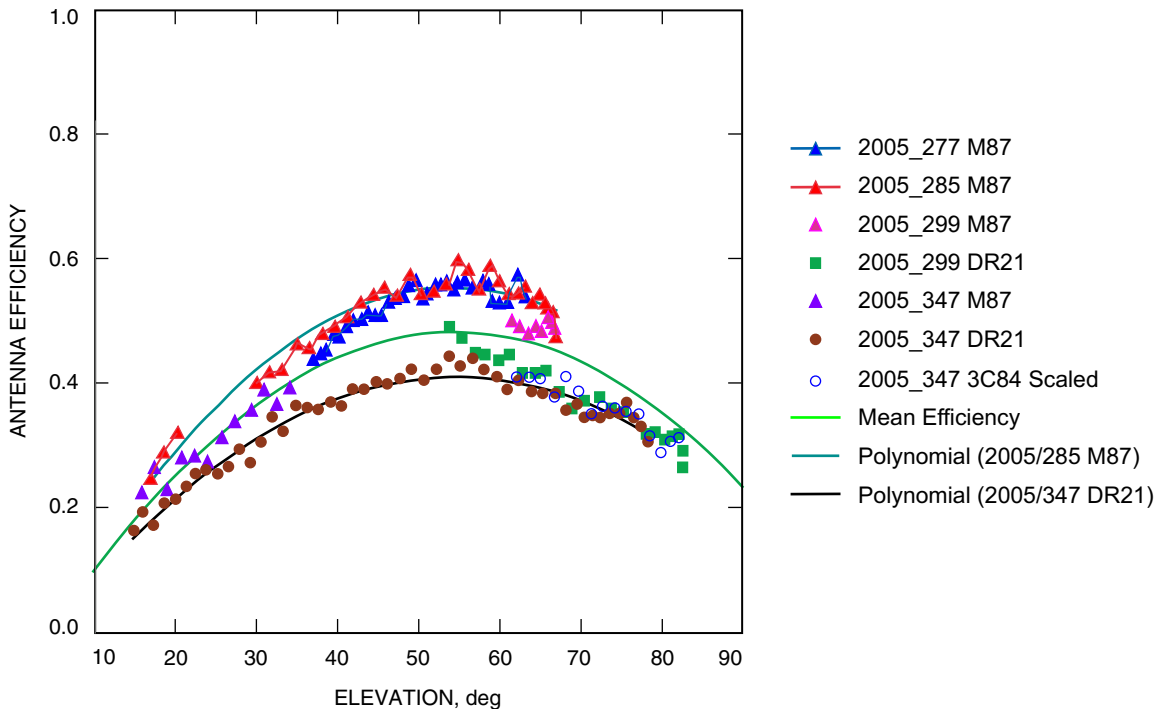


Fig. 2. DSS-13 Ka-band efficiency data acquired during several measurement sessions, along with fitted curves.

⁵ M. J. Klein, personal communication, Jet Propulsion Laboratory, Pasadena, California, 2004.

signal power. The initial measurements performed on October 12–13, 2005, and October 26–27, 2005, displayed significantly reduced efficiency (35 to 55 percent) compared to earlier estimates (~ 70 percent) performed at this feed position [4] and also showed a hysteresis-like signature that was not previously present. This was attributed to the new package that was installed in July 2005 for the Faraday rotation experiment that did not require a comprehensive alignment. The efficiency curve derived from these data was used for the initial X-band MRO observations until the X-band package was realigned on 2005/320, after which additional efficiency data were acquired. Improved efficiency of nearly 70 percent was realized but still with a small amount of hysteresis (Fig. 3).

IV. Procedures for Measuring Received Signal Strength and EIRP

During the period shortly after launch, a deep-space probe usually communicates with Earth using its LGAs as there is more than sufficient signal strength for communications links that use low engineering data rates—from hundreds to a few thousand bits per second (bps). At some later point, the HGA is deployed for communications, when the LGA can no longer support the required communications data rates or when high data rates are required. For the MRO Ka-band demonstration, it was desired that Ka-band functionality be verified as soon as was possible after launch, and this could only be done using the HGA. The HGA being deployed within only a few weeks after launch resulted in high signal strengths that saturated the DSN receivers and made measurement of T_{op} problematic.

Although the Ka-band telemetry, Doppler, and range were received nominally, it was necessary to verify that the HGA was on-point shortly after the HGA calibration, and this could only be done by accurately measuring EIRP. The R&D station DSS 13 was well-suited for this task, but the system was not optimal early in the campaign. Starting in November 2005, steps were taken to upgrade the system to enable it to measure EIRP accurately. This included securing an adequate filter that accommodated MRO’s high IF frequency at Ka-band for use at the TPR, and performing a series of calibrations, measurements, and tests to ensure system linearity and the ability of the system to accurately measure received signal strength.

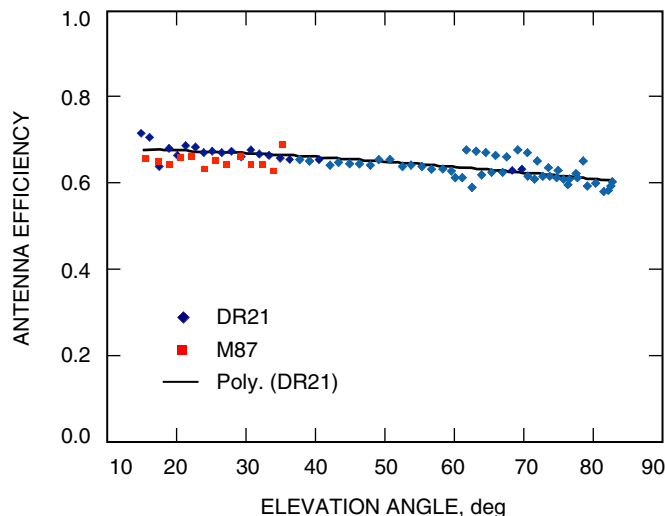


Fig. 3. X-band efficiency curve for the case where the antenna is peaked at Ka-band during the AUTOBORE sequence (note the hysteresis above the 60-deg elevation angle).

A set of procedures was developed and exercised to measure signal strength using the TPR and the station spectrum analyzers. The latter entailed measurement of carrier peak minus noise floor, or the carrier peak strength referenced to the LNA input using system gain calibrations. The simultaneous observation of X-band and Ka-band was made possible by the use of a dichroic plate at DSS 13. Figure 4 displays a block diagram of the Ka-band signal path from the input of the LNA to the TPR, as well as to other equipment.

A. TPR Method

This section describes the TPR method of measuring EIRP. The TPR accepts two independent IF signal paths, usually one from X-band RCP and the other from Ka-band RCP, for the case of MRO. In general, the measurement of the T_{op} increase at elevation angle θ is expressed as

$$\Delta T(\theta) = T_{\text{op,on-source}}(\theta) - T_{\text{op,off-source}}(\theta) \quad (1)$$

where the on-source and off-source values are taken over a short measurement period at the same position in the sky, and θ is the station elevation angle. The on-source measurement is performed after the antenna is peaked on the signal source using the AUTOBORE or manual boresight algorithm. The off-source measurement is usually done in cross-elevation angle sufficiently far away from the signal source such that elevation-angle-dependent atmospheric effects are minimized. In some cases it was necessary to move 10-deg off-source in cross-elevation because the MRO signals were so strong that they caused the antenna side lobes to pick up appreciable signal energy at smaller offsets. Because the measurement sequence is performed regularly over a pass, the elevation-angle dependence is effectively removed and, therefore, does not require modeling (other than performing a fit over the off-source noise temperature measurements). The received signal strength can then be estimated by using

$$P_r = k \Delta T B \quad (2)$$

where ΔT is given in Eq. (1), k is Boltzmann's constant, and B is the equivalent noise bandwidth of the system. The received signal strength can be compared with predicts using the link equation usually provided by programs such as Telecom Forecast Predictor (TFP) [5].

A specialized filter was required in order to accept MRO's Ka-band 522-MHz IF signal within a reasonably small bandwidth in the Ka-band equipment chain. The filter was placed just before the TPR power meter such that stray noise effects outside the bandwidth from other components did not corrupt the measurements. The filter's frequency response is displayed in Fig. 5. It has an insertion loss of 3.6 dB, a center frequency of 524 MHz, a noise equivalent bandwidth of $B = 13.3$ MHz [for use in Eq. (2)], and roll-off (in the stop band) of 4 dB/MHz. This filter was utilized as a prime component in the MRO Ka-band EIRP measurements using the TPR method. The center frequency and bandwidth of this filter were such that the filter can accept all of the power in MRO's Ka-band signal, including carrier and telemetry.

Once the received signal power [Eq. (2)] is measured, it can be referred to the spacecraft by correcting for all other link contributions between the station and the spacecraft to yield EIRP at the spacecraft. The EIRP measurement can be compared with predictions and provides an indication of how well the spacecraft is performing or of any problem at the spacecraft, such as mispointing of the HGA. Thus, EIRP (in watts) can be estimated from received signal power by removing the effects due to space loss, atmospheric attenuation, gain of the receiving antenna, and miscellaneous losses such as depolarization and ground mispointing:

$$\text{EIRP} = P_r \left(\frac{\lambda}{4\pi r} \right)^{-2} L_a^{-1} L_c^{-1} G_r^{-1}(\theta) \quad (3)$$

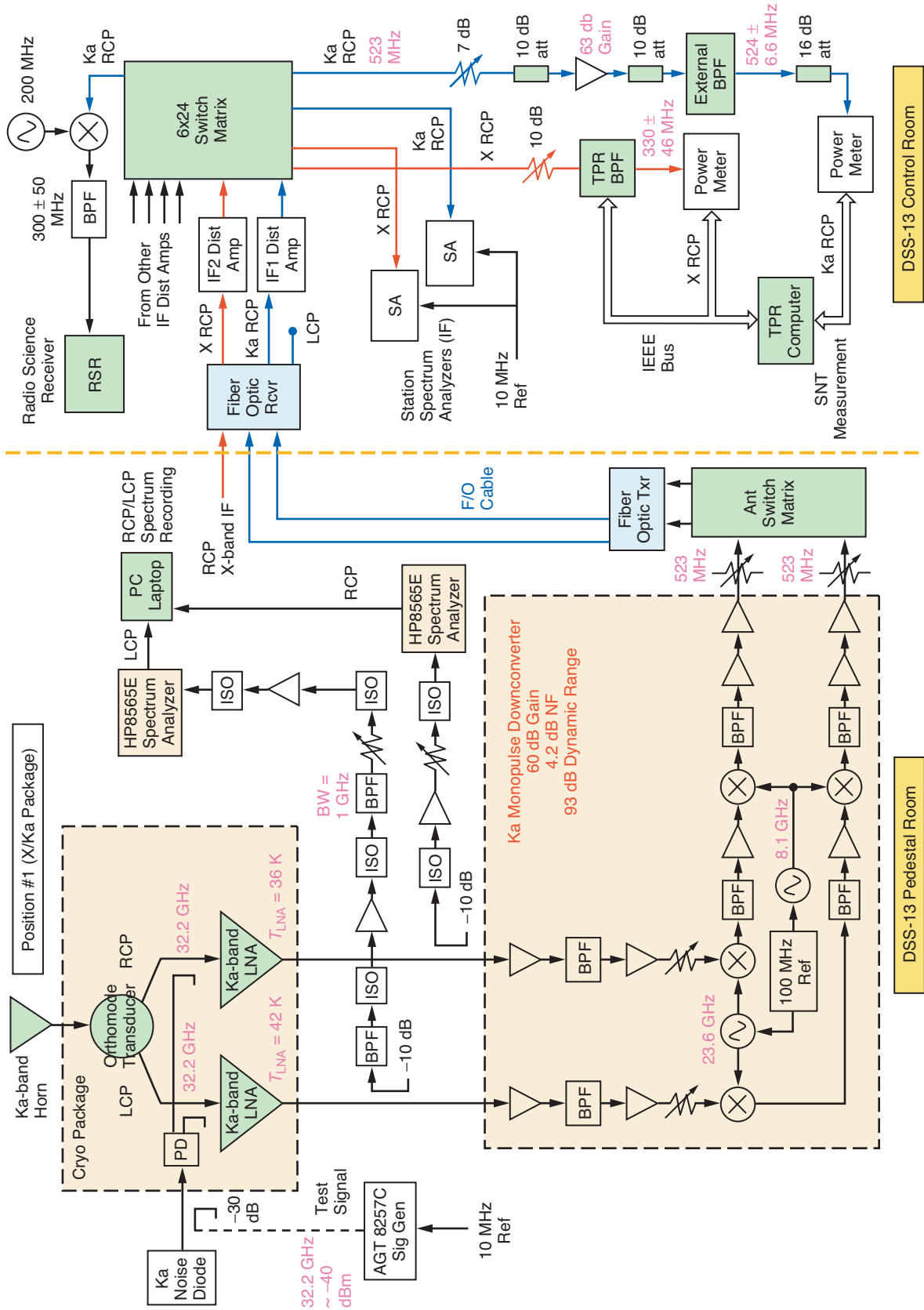


Fig. 4. Configuration of Ka-band signal paths at DSS 13.

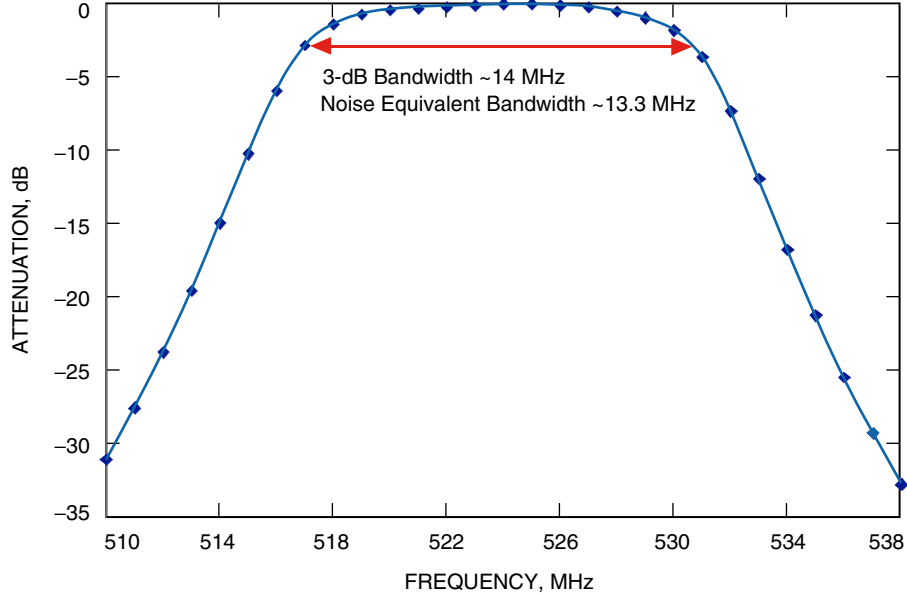


Fig. 5. Frequency response of the bandpass filter used as the external filter input to the TPR for MRO Ka-band.

where

P_r = received signal power at the ground station [Eq. (2)]

λ = signal wavelength

r = spacecraft-to-station range distance

L_a = atmospheric attenuation, >1

L_c = lumped miscellaneous losses such as circuit losses, >1

G_r = ground station antenna gain (ratio >1), which is a function of elevation angle, θ

The gain of the receiving antenna employs the antenna efficiency curves previously discussed (Section III). The atmospheric attenuation (L_a) can be calculated using surface meteorological parameters input into a weather model⁶ or from a tip curve of the off-source T_{op} .

B. Station Spectrum Analyzer Method at IF Using Carrier Peak and Noise Floor

Measurements of carrier power at IF were performed using the station spectrum analyzer in the DSS-13 control room by peaking onto the spectrum analyzer carrier power, $(P_c)_{SA}$ (assume noise power is negligible compared to carrier power). The antenna was then moved off-source in cross-elevation angle by at least 5 to 10 deg, and the noise floor, $(P_n)_{SA}$, was measured. Given the resolution bandwidth (RBW) of the station spectrum analyzer setting, the received carrier power-to-noise spectral density was given by

$$\left(\frac{P_c}{N_0}\right)_{SA} = \frac{(P_c)_{SA}}{(P_n)_{SA} \text{ RBW}} \quad (4)$$

⁶S. D. Slobin, Jet Propulsion Laboratory, Pasadena, California, 2005, provided the weather model that uses surface meteorological data as input.

By measuring the off-source T_{op} using the TPR, the received P_c/N_0 in Eq. (4) can be converted to received signal power, P_r , referenced to the point in the system where calibrations are performed. In addition, when telemetry modulation was present on the carrier, P_r was estimated by correcting for the telemetry modulation index, θ_{tlm} . The following [Eq. (5a)] assumes that ranging is turned off:

$$P_r = \frac{\left(\frac{P_c}{N_0}\right)_{\text{SA}} k T_{\text{op}}}{\cos^2(\theta_{\text{tlm}})} \quad (5a)$$

If sine wave ranging was used with a ranging modulation index, θ_r , the total signal power can be estimated, assuming high uplink ranging signal-to-noise ratio (SNR), using

$$P_r = \frac{\left(\frac{P_c}{N_0}\right)_{\text{SA}} k T_{\text{op}}}{\cos^2(\theta_{\text{tlm}}) J_0^2(\theta_r)} \quad (5b)$$

The spacecraft EIRP is then computed using P_r from Eqs. (5a) and (5b) in Eq. (3).

C. Station Spectrum Analyzer Method at IF Using Carrier Peak and System Gain

This technique involves measuring the peak carrier power at the spectrum analyzer, P_c , and referencing it back to total power at the front-end of the antenna using the system gain, G_{sys} , measured by the TPR. The system gain was measured while on ambient load (power versus calibration-load physical temperature with appropriate corrections). Because the path from the IF distribution amplifier to the station spectrum analyzer was different from the path to the TPR, the gain difference between the two paths, ΔG , was calibrated and used to adjust the system gain. Accounting for the telemetry modulation index, θ_{tlm} , the received power at the antenna, P_r , based on spectrum analyzer measurement of the IF carrier power, P_{CSA} , was calculated as follows:

$$P_r = \frac{(P_c)_{\text{SA}}}{G_{\text{sys}} \Delta G \cos^2(\theta_{\text{tlm}})} \quad (6)$$

The spacecraft EIRP was then computed using P_r from Eq. (6) in Eq. (3).

D. Station Spectrum Analyzer Method at Radio Frequency

The final technique used to estimate the spacecraft EIRP was a direct radio frequency (RF) spectrum measurement at Ka-band. This involved adding two 10-dB couplers to the waveguide segment connecting the RCP/LCP LNA outputs to the Ka-band downconverter (see Fig. 4), which allowed RF spectrum measurements to be conducted without interrupting the TPR or IF spectrum measurements. Due to the relatively low signal power at RF (-110 dBm), two external RF amplifiers were employed after the couplers to boost the signal power into the spectrum analyzers. In addition, bandpass filters were employed to filter out some of the noise. The test setup included two HP 8565E spectrum analyzers (0 to 50 GHz), with one connected to the RCP signal and the other connected to the LCP signal. Through the general purpose interface bus (GPIB) interface, the outputs of the spectrum analyzers were logged onto a laptop computer for future analysis. The received power from the spacecraft, P_r , was computed using the measured carrier-to-noise-spectral-density ratio, P_c/N_0 , on the spectrum analyzer in Eq. (5a). Using Eq. (3), P_r was then translated into an estimate of the spacecraft EIRP.

V. Activities and EIRP Measurements Performed on December 16, 2005 (2005/350)

A. Ka-Band Activities

This section describes activities and measurements performed on December 16, 2005 (2005/350) at DSS 13. From about 3:30 to about 7:00 UTC (universal time constant), a series of calibrations, measurements, and tests was performed in the pedestal room (RF) and control room (IF). From about 7:00 to 10:00 UTC, the MRO spacecraft was tracked at X-band and Ka-band while measurements were being made at RF and IF. Measurements of signal EIRP at IF used the TPR and station spectrum analyzers (Sections IV.A and IV.B) in the DSS-13 control room. In addition, EIRP measurements at RF were performed in the DSS-13 pedestal room at the Ka-band front-end (Section IV.D). Prepass activities included setting up an RF measurement station inside the pedestal room and conducting measurements characterizing system response and linearity in the pedestal room at RF and in the control room at IF. A signal (sine wave) was injected into the noise diode port of the Ka-band LNA with a 10-dB coupler. The RF measurements were extracted at the output of the LNA (see Fig. 4). Inside the control room, concurrent measurements were performed at IF using the TPR and spectrum analyzer (see Fig. 6). During this test, the increase in T_{op} as a function of injected signal generator power was also measured. These results (see Fig. 7) indicate that the system was remarkably linear for T_{op} up to several thousand kelvins. The T_{op} increase of MRO's Ka-band signal ranged between 100 K and 350 K on 2005/350, well within the linear region.

The T_{op} recorded by the TPR is usually sampled every 5 seconds. From about 7:00 to 10:00 UTC, the MRO spacecraft was tracked at X-band and Ka-band while measurements were being made at RF (in the pedestal room) and IF (in the control room). During this period, system calibrations, AUTOBOREs, and on-source and off-source T_{op} measurements were performed. The calibrations were performed periodically to calibrate total power with an ambient load source and to measure linearity of the system. The AUTOBORE observations were conducted periodically to peak the pointing onto the source. The series of on-source and off-source T_{op} measurements were then used to evaluate ΔT in Eq. (1). Figure 8 depicts the on-source and off-source T_{op} measurements acquired on 2005/350 (data acquired during prepass activities, calibrations, and AUTOBOREs have been removed). During the measurement period in Fig. 8, the station elevation angle of the MRO spacecraft changed from 50 deg down to 10 deg.

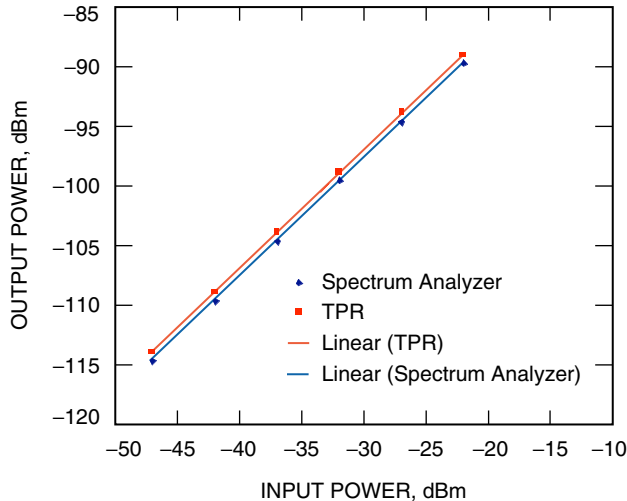


Fig. 6. Output power during 2005/350 measured at the TPR and station spectrum analyzer at IF versus injected input signal power. Output power was measured in the DSS-13 control room.

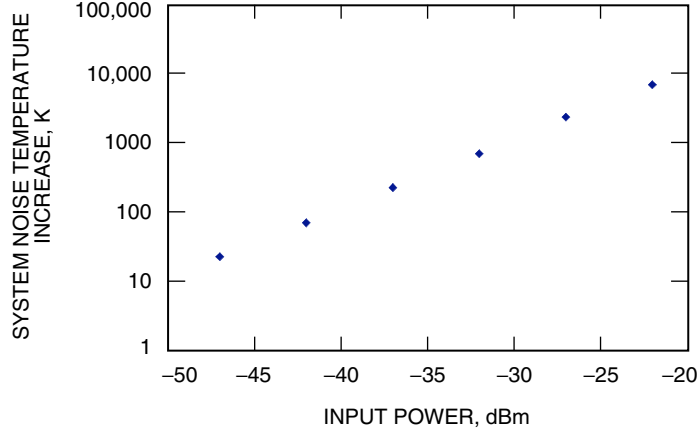


Fig. 7. ΔT_{op} increase measured at the TPR during the signal injection test in log scale versus input power.

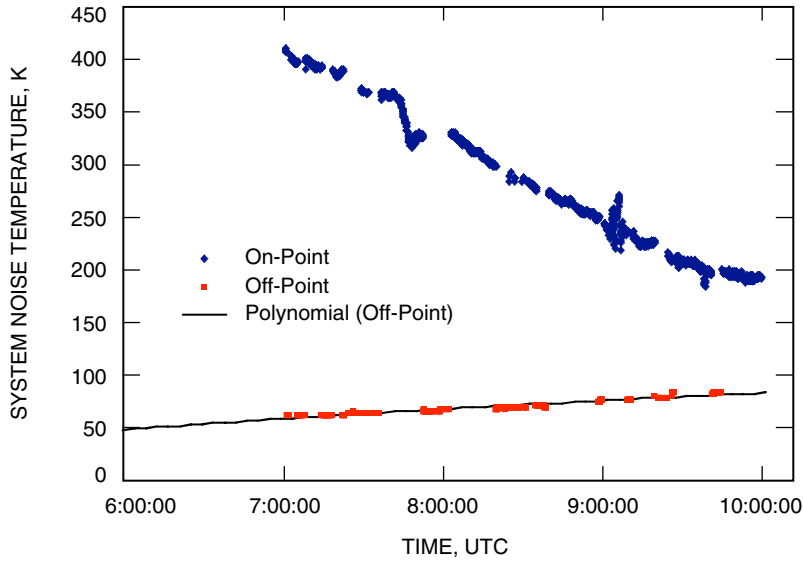


Fig. 8. TPR data peaked on-source (MRO Ka-band signal) and off-source acquired on 2005/350, along with the off-source fitted curve.

In Figure 8, the off-source and on-source data are disjoint. A polynomial fit was performed on the off-source data and then differenced from the on-source data to yield ΔT_{op} due to the MRO Ka-band spacecraft signal [Eq. (1); see Fig. 9]. In Fig. 9, note the significant span in ΔT_{op} from 350 K to about 100 K. This large decrease is attributed to elevation dependence of both the antenna efficiency and atmosphere at Ka-band.

The ΔT_{op} signature depicted in Fig. 9 was converted to received signal power using the TPR method, Eq. (2). The resulting received signal power is displayed in Fig. 10 in blue. Also shown in Fig. 10 are measurements using the spectrum analyzer methods (red squares are spot checks at IF; green squares are measurements at RF). There was also agreement with measurements using the 6-m prototype array

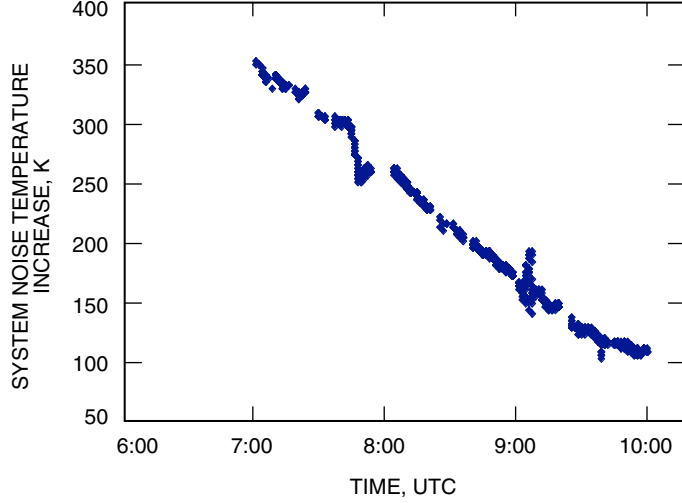


Fig. 9. ΔT_{op} of the MRO Ka-band signal at DSS 13 on 2005/350.

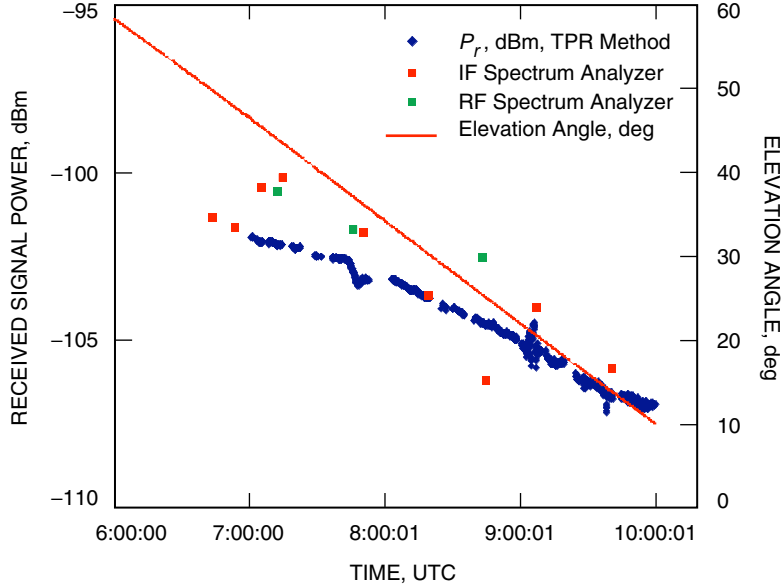


Fig. 10. Measured Ka-band received signal strength on 2005/350.

breadboard antennas⁷ (after correcting for differences in antenna size and efficiency). The uncertainty of the spectrum analyzer measurements is large due to errors in visually selecting a value for the noise floor, $(P_n)_{\text{SA}}$ in Eq. (4).

Finally, using Eq. (3), the received signal power measurements in Fig. 10 were converted to EIRP referenced at the plane of the spacecraft HGA and are shown in Fig. 11. The solid red line in Fig. 11 denotes the predicted EIRP assuming the spacecraft HGA is perfectly Earth-pointed. The EIRP measurements mostly lie within 1 dB of the predictions and display some interesting signatures. The large second-order effect could be attributed to a deficiency in the efficiency-model assumption or spacecraft

⁷S. Weinreb, M. Britcliffe, and H. Cooper, personal communication, Jet Propulsion Laboratory, Pasadena, California, 2005.

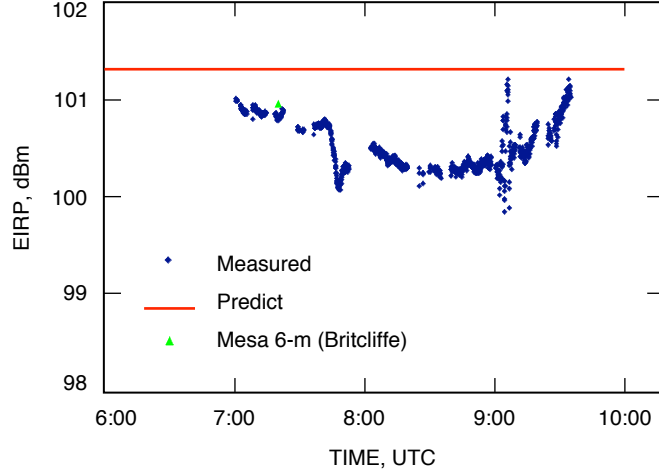


Fig. 11. MRO Ka-band EIRP on 2005/350 referenced at the spacecraft and prediction (101.3 dBm).

motion. There are some other signatures on shorter time scales that are not yet understood. The error sources in the Ka-band EIRP estimates include measurement noise of ~ 0.1 K over a 5-s integration time. The uncertainty in the efficiency curve is anticipated to be ± 0.6 dB, is mostly systematic, and is a very conservative worst-case estimate. Atmospheric attenuation was about 0.41 ± 0.03 dB (at 20-deg elevation), with small relative uncertainty (depicted in the red-line elevation-dependent tip-curve model of Fig. 12). Spacecraft mispointing and polarization loss are not characterized. Presumably spacecraft mispointing can be characterized by the difference of the prediction (red curve) and measurements (blue points) in Fig. 11. System nonlinearity of about 2 to 3 percent is expected to translate to less than 0.2 dB in the error budget.

Figure 12 represents a record of the off-source T_{op} measurements during the pass as a function of elevation angle. This record can be treated as a “tip curve” from which atmospheric optical depth was calculated using the elevation-angle dependence. The atmospheric noise temperature and atmospheric attenuation can then be calculated from the optical depth and used in the telecommunications link model as a function of elevation angle. In the absence of a tip curve with sufficient elevation angle swing, the parameters could alternatively be estimated from a surface model⁸ with input meteorological data. The estimate of optical depth using the surface model agreed with that derived from the tip curve of Fig. 12 ($\tau = 0.033 \pm 0.002$).

B. X-Band Activities

The same techniques were used to estimate X-band EIRP. A record of the T_{op} measured at DSS 13 on 2005/350 for MRO’s X-band signal while on-source and off-source is displayed in Fig. 13. The ΔT_{op} measurements obtained from the data in Fig. 13 were then converted to estimates of received signal power, which in turn were converted to estimates of EIRP using the equations provided in Section IV.A. The X-band EIRP measurements in Fig. 14 lie below the predicted value by 0.5 dB, with less than ~ 0.2 dB of fluctuation about the mean value.

Figure 15 displays simultaneous X-band and Ka-band EIRP (on different scales), showing detail on the respective signal variations for comparison. Note there are some correlations, such as that of the features occurring after 7:41 UTC. The X-band takes a rapid 0.3-dB decrease near 7:40 UTC whereas Ka-band

⁸S. D. Slobin, personal communication, Jet Propulsion Laboratory, Pasadena, California, 2005.

takes a 0.7-dB decrease during this same time period. The unusual signatures from 7:43 to 7:53 UTC for both X-band and Ka-band appear correlated but do not follow strict wavelength dependence for either the HGA or the BWG. There appear to be variations elsewhere with interesting signatures in both X-band and Ka-band, which are not necessarily correlated.

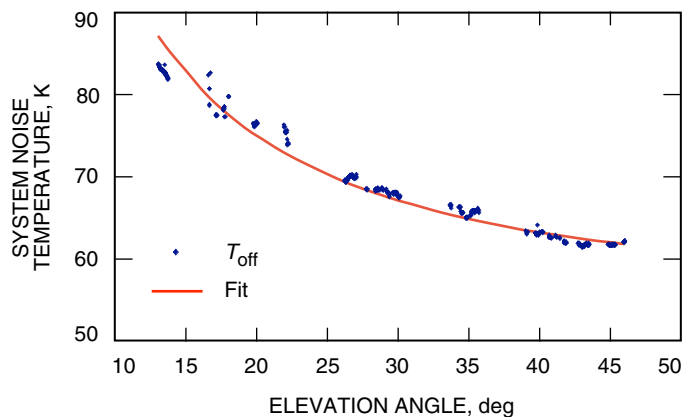


Fig. 12. Off-source (cold-sky) T_{op} versus elevation angle used as a tip curve to provide an estimate of atmospheric attenuation along with the fitted model.

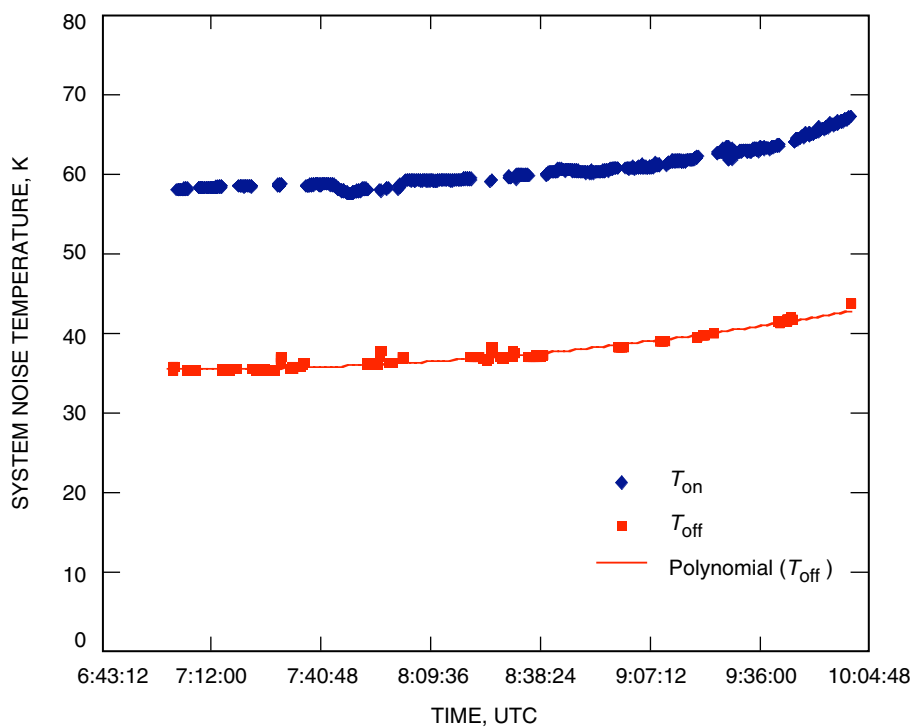


Fig. 13. MRO X-band on-source and off-source T_{op} along with fitted curve of off-source T_{op} .

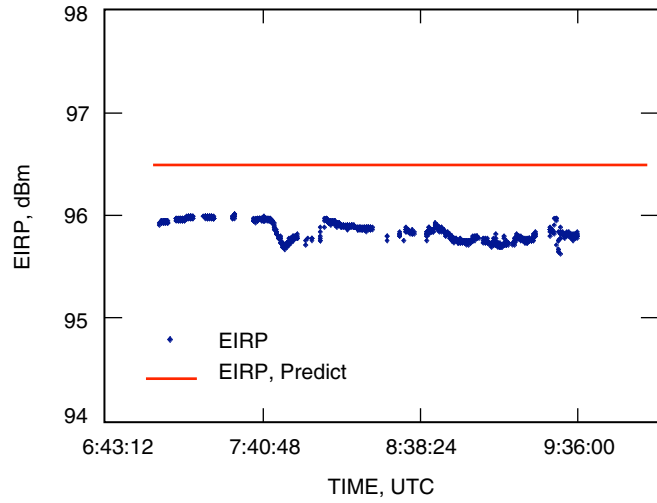


Fig. 14. Measured X-band EIRP with predict (96.5 dBm).

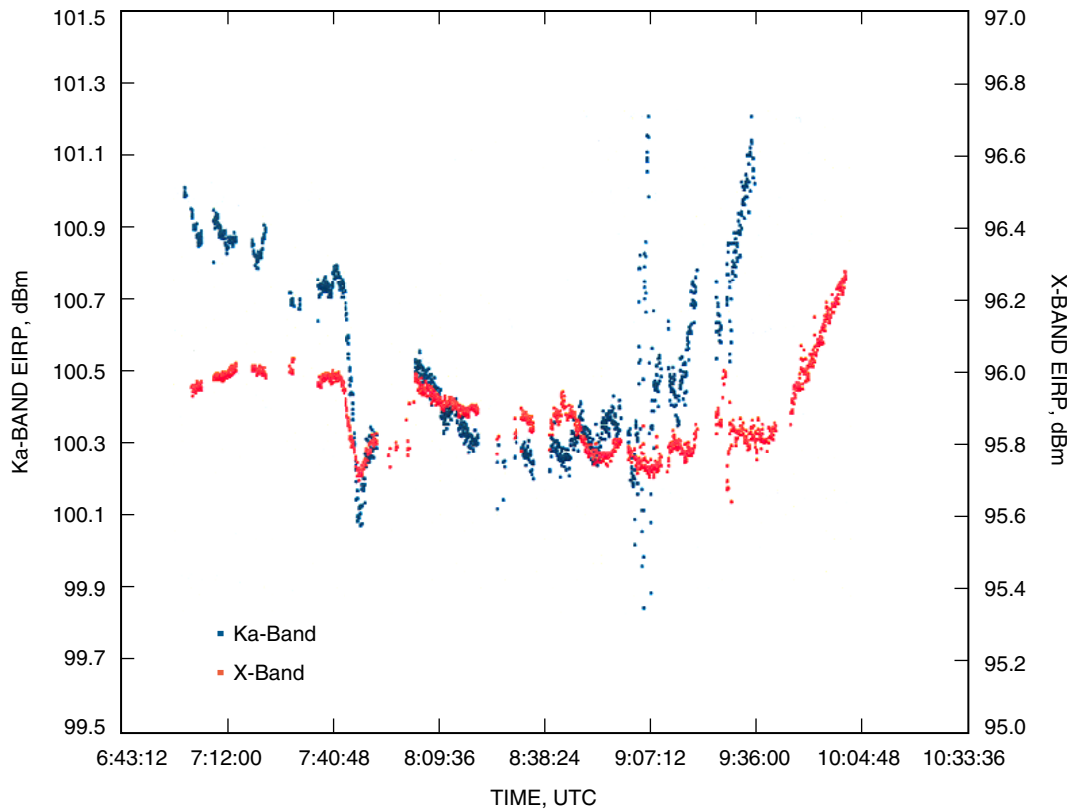


Fig. 15. Measured X-band and Ka-band EIRP at DSS 13 during 2005/350.

VI. Overall EIRP Measurement Set

Figure 16 displays Ka-band EIRP measured at DSS 13 during a pass conducted on December 22, 2005 (2005/356), using the same TPR technique, except that the T_{op} increase, ΔT in Eq. (1), is now obtained from the AUTOBORE program output in both orthogonal directions. Notice that there is general agreement between the two Ka-band measurement sets (Figs. 11 and 16), and the measurements mostly lie within 1 dB of the predicted EIRP. There is an unexplained dip near 03:00 UTC in Fig. 16.

In addition to the 2005/350 and 2005/356 tracks, there were other tracks conducted with the goal of measuring Ka-band EIRP, as summarized in Fig. 17. The red diamonds in Fig. 17 were measurements performed at the 6-m prototype array antennas located on the Mesa at JPL.⁹ These antennas used MRO's X-band and Ka-band signals for the dual purposes of providing EIRP measurements and of verifying antenna performance and identifying problems. All of the DSS-13 measurements utilized filters at the TPR input to the power meters, or spectrum analyzer measurements using procedures described in Section IV. Note that there is good agreement between the measurements, all consistent with MRO being on-point. One measurement conducted in early January was found to be several decibels low, but it was later determined to be due to spacecraft mispointing caused by an out-dated ephemeris that was loaded in shortly after a safing event on January 3, 2006. The pointing error attributed to the ephemeris was found to be consistent with the observed degradation, and EIRP was corrected using the known off-point angle of 0.095 deg for this date.¹⁰ This degradation was expected to decrease as the spacecraft approached Mars.

A measurement conducted on December 8, 2005 (2005/342), used a third local oscillator (LO)/mixer and filter inserted in the IF chain to bring the MRO Ka-band signal down to an IF near 322 MHz instead of using the specialized 522-MHz filter. This measurement is consistent with the on-point predicted value

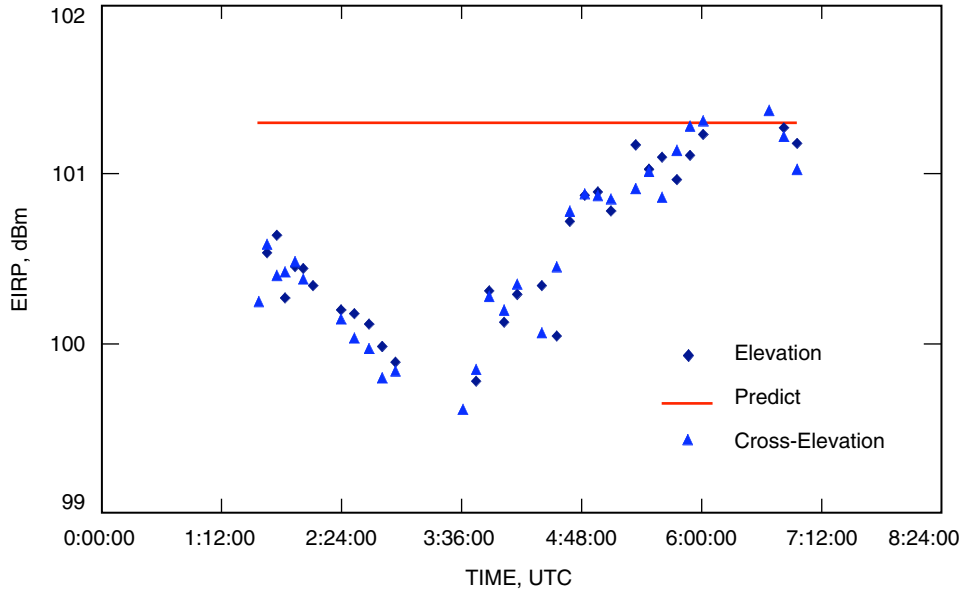


Fig. 16. Ka-band EIRP during 2005/356 using the TPR method with AUTOBORE data and predicted EIRP.

⁹ S. Weireb, M. Britcliffe, and H. Cooper, personal communication, Jet Propulsion Laboratory, Pasadena, California, 2005.

¹⁰ D. Skulsky, personal communication, Jet Propulsion Laboratory, Pasadena, California, January 16, 2006.

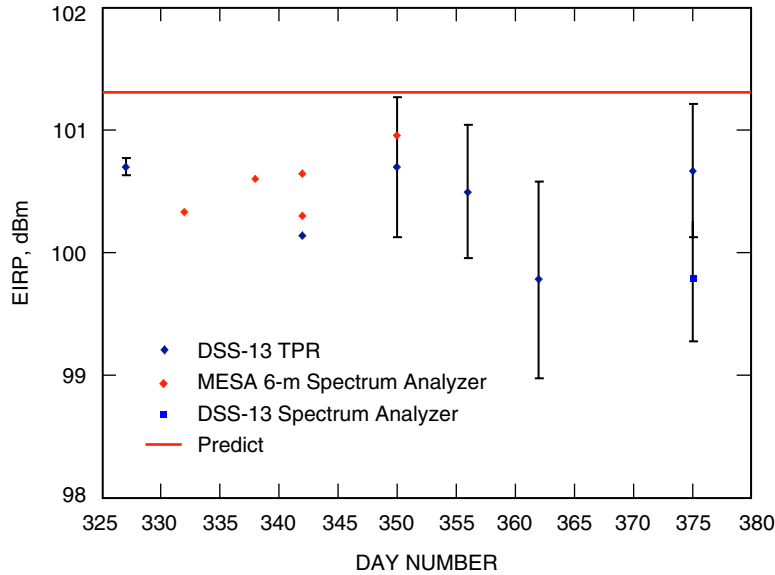


Fig. 17. DSS-13 and JPL Mesa Ka-band measurements of MRO Ka-band EIRP and prediction (101.3 dBm).

and also involved placing a standard narrowband station filter prior to the TPR power meter. The plotted point for November 23, 2005 (2005/327), was the first attempt to use the 522-/13.3-MHz narrowband filter at DSS 13.

Earlier attempts to measure EIRP in September and October 2005 were plagued by the DSN's receivers being saturated by excessive received signal power due to the short range of the spacecraft while on the HGA. In addition, the operational DSN was unable to measure T_{op} under such conditions. Early attempts to measure EIRP at DSS 13 in October and November 2005 were not successful because of the nonoptimal system that was in place at the time. The system was nonlinear at the 10 percent level, and there were no suitable filters at the TPR to accommodate the MRO signal frequency (32.222 GHz) at the high end of the IF passband near 522 MHz. After appropriate equipment was procured (filters) and appropriate placement of attenuation and amplification was performed, consistent measurements were achieved, and they compared favorably with those taken at the 6-m array on the JPL Mesa.

The measurement set of Fig. 17 confirmed that the MRO Ka-band EIRP measured at DSS 13 was consistent with the HGA being on-point, within about 1 dB of predictions. The error bars on the DSS-13 measurements represent the standard deviation of the TPR measurements about the mean value over each pass, except for one short "spot check" measurement where the error bar was given a value of 0.5 dB to account for unknown effects.

VII. Conclusion

A measurement campaign at DSS 13 was conducted during the fall and winter of 2005 for the purposes of characterizing the EIRP of MRO and exercising several EIRP measurement techniques. The Ka-band measurements indicate that the MRO HGA was on-point and were supported by similar measurements conducted using the JPL Mesa 6-m prototype array antennas. Earlier attempts to measure EIRP at DSS 13 in October and November 2005 were plagued by several problems that have since been addressed.

Acknowledgments

We would like to thank Paul Dendrenos, William Lake, and Ron Littlefair for providing support in conducting tests, measuring RF system parameters, and supporting the measurement sessions; Ron Littlefair for also addressing MRO printing issues; Gary Bury and Bob Rees for coordinating station support; Kamal Oudrhiri, Sue Finley, Sami Asmar, and Andre Jongeling for their consultation and expertise in RSR related matters; and Sander Weinreb, Mike Britcliffe, and Hamil Cooper for providing and measuring EIRP using the Mesa 6-m antennas. We would also like to thank other participants who assisted in the activity at DSS 13 on 2005/350, including Brad Arnold, Sam Zingales, and Stan Butman.

References

- [1] F. Davarian, S. Shambayati, and S. Slobin, "Deep Space Ka-Band Link Management and Mars Reconnaissance Orbiter: Long Term Weather Statistics versus Forecasting," *Proceedings of the IEEE*, vol. 92, issue 12, pp. 1879–1894, December 2004.
- [2] S. Shambayati, D. Morabito, J. Border, F. Davarian, D. Lee, R. Mendoza, M. Britcliffe, and S. Weinreb, "Mars Reconnaissance Orbiter Ka-band (32 GHz) Demonstration: Cruise Phase Operations," *The Proceedings of the AIAA SpaceOps 2006 Conference*, Rome, Italy, June 19–24, 2006.
- [3] C. Stelzried and M. Klein, "Precision DSN Radiometer Systems: Impact on Microwave Calibrations," *Proceedings of the IEEE*, vol. 82, pp. 776–787, May 1994.
- [4] D. D. Morabito, "The Characterization of a 34-Meter Beam-Waveguide Antenna at Ka-band (32 GHz) and X-band (8.4 GHz)," *IEEE Antennas and Propagation Magazine*, vol. 41, no. 4, pp. 23–34, August 1999.
- [5] K. K. Tong and R. H. Tung, "A Multimission Deep-Space Telecommunications Analysis Tool: The Telecom Forecaster Predictor," *The Telecommunications and Mission Operations Progress Report 42-140, October–December 1999*, Jet Propulsion Laboratory, Pasadena, California, pp. 1–7, February 15, 2000.
http://ipnpr/progress_report/42-140/140C.pdf